Out-of-plane losses of two-dimensional photonic crystals waveguides: electromagnetic analysis

Philippe Lalanne, Henri Benisty

Out-of-plane losses of two-dimensional photonic crystals waveguides: Electromagnetic analysis

Ph. Lalanne[a)]
Laboratoire Charles Fabry de l'Institut d'Optique, CNRS, BP 147, 91 403 Orsay Cedex, France

H. Benisty
Laboratoire de Physique de la Matière Condensée, Ecole Polytechnique, UMR 6743 du CNRS, 91128 Palaiseau Cedex, France

(Received 17 July 2000; accepted for publication 16 October 2000)

A method for the electromagnetic analysis of photonic crystal waveguides is described. It is tested against experimental transmission data obtained for AlGaAs slab-waveguide structures perforated by a two-dimensional hexagonal lattice. A good quantitative agreement is obtained for the band edge locations, for the ripples in the transmission windows, and more importantly, for the out-of-plane losses induced by the finite hole depth. The ultimate performance of the structure for deep etched holes is predicted. © *2001 American Institute of Physics.* [DOI: 10.1063/1.1331331]

Photonic crystals are artificial optical materials, whose dielectric constant presents a strong periodic modulation. The modulation offers the possibility of controlling and manipulating light by opening a photonic band gap within a given range of frequencies. Because of the challenge to fabricate three-dimensional (3D) photonic crystals with submicronic feature sizes, much efforts are devoted to the fabrication of two-dimensional (2D) photonic crystal etched through waveguides. These waveguides, called hereafter ICPC for index-confined photonic crystals, are a promising substitute to conventional planar lightwave circuits.[1] Experimentally, reflection, transmission, and propagation through semiconductor-based ICPC have been demonstrated at near-infrared wavelengths.[2–6] The analysis of ICPC is often performed with 2D band gap calculations of crystals with infinite depth, thereby ignoring the vertical confinement.

Although computation plays a crucial role in such analysis because Maxwell's equations for linear dielectric materials are exact, methods for modeling ICPC are not common in the literature. With the exception to the work of Ref. 7, where finite-difference time-domain methods are used to determine *indirectly* the modal reflectivity of ICPC through the computation of microcavity quality factors, no 3D modeling of the propagation through ICPC have been reported.

The method proposed here belongs to the general class of frequency-domain modal methods. It is inspired from crossed grating theory[8] in the sense that Fourier series are used to expand the electromagnetic modes, but its novelty consists in extending these theories to waveguided geometries. A 2D example of a similar extension is proposed in Ref. 9. Figure 1 shows one possible ICPC geometry that will be used here to illustrate the method. The ICPC is assumed to be periodic in the x direction (period Λ_x) and to have a finite spatial extent into the z direction. The y direction is normal to the dielectric stack. The corrugated waveguide is assumed to be illuminated from the input unpatterned region by the fundamental TE_0 or TM_0 mode under an incidence angle θ. We denote by k_x the x component of the mode wave vector. The wavelength in the vacuum of the incident light is $\lambda (k_0=\omega/c=2\pi/\lambda)$.

In the orthogonal Cartesian coordinate (x,y,z) system, the curl Maxwell equations in the Gaussian system of units are $\mathbf{curl}\ \mathbf{H}=-i\omega/c\,\boldsymbol{\epsilon}(\mathbf{r})\mathbf{E}$ and $\mathbf{curl}\ \mathbf{E}=i\omega/c\mathbf{H}$. $\mathbf{H}$ and $\mathbf{E}$ are the magnetic and electric fields and $\boldsymbol{\epsilon}$ is the relative permittivity. Due to periodicity along the x direction, a pseudoperiodic plane-wave basis can be used for the x expansions of $\mathbf{E}$ and $\mathbf{H}$ (Floquet or Bloch theorem). Following Ref. 9, we introduce an artificial periodization with absorbing boundaries along the y direction [period Λ_y, see Fig. 2] and use a plane-wave y expansion for the electromagnetic fields. Thus, $\mathbf{H}$ and $\mathbf{E}$ are written

$$\mathbf{H}=\sum_{l,m}(U_{xlm}\mathbf{x}+U_{ylm}\mathbf{y}+U_{zlm}\mathbf{z})\exp i[(k_x+lG_x)x+mG_y y] \tag{1a}$$

$$\mathbf{E}=\sum_{l,m}(S_{xlm}\mathbf{x}+S_{ylm}\mathbf{y}+S_{zlm}\mathbf{z})\exp i[(k_x+lG_x)x+mG_y y], \tag{1b}$$

where $G_\alpha=2\pi/\Lambda_\alpha$ and the $S_{\alpha lm}$ and $U_{\alpha lm}$ ($\alpha=x$, y, or z) are z-dependent coefficients. In the following, we denote by $\mathbf{K}_{lm}$ the vector equal to $(k_x+lG_x)\mathbf{x}+mG_y\mathbf{y}$. By incorporating expressions (2a) and (2b) into the curl equations and by expanding the equations in the plane-wave basis, we obtain

$$\frac{1}{k_0}\frac{d[\boldsymbol{\Psi}]}{dz}=\begin{bmatrix}\mathbf{0} & \mathbf{0} & \mathbf{K_yK^{-1}K_x} & \mathbf{1-K_yE^{-1}K_y}\\ \mathbf{0} & \mathbf{0} & \mathbf{K_xE^{-1}K_x-I} & \mathbf{-K_xE^{-1}K_y}\\ \mathbf{K_xK_y} & \boldsymbol{\epsilon}_\mathbf{x}\mathbf{-K_y^2} & \mathbf{0} & \mathbf{0}\\ \mathbf{K_x^2-}\boldsymbol{\epsilon}_\mathbf{y} & \mathbf{-K_xK_y} & \mathbf{0} & \mathbf{0}\end{bmatrix}\times[\boldsymbol{\Psi}], \tag{2}$$

where $\boldsymbol{\Psi}$ is equal to $[\mathbf{S}_y\mathbf{S}_x\mathbf{U}_y\mathbf{U}_x]^t$, a column vector formed by the electric- and magnetic-field coefficients. In Eq. (2), $\mathbf{K}_x$

a)Electronic mail: philippe.lalanne@iota.u-psud.fr

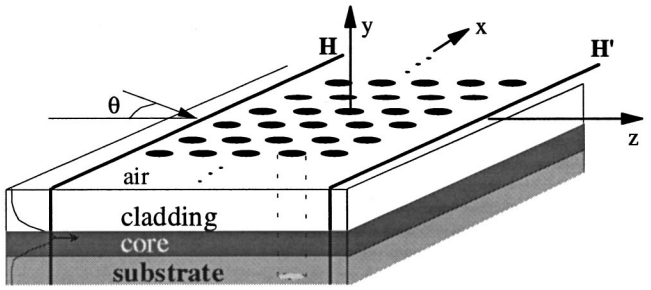

FIG. 1. ICPC geometry. The structure is periodic in the *x*-direction, has a finite arbitrary extent in the *z* direction and is illuminated by the fundamental mode of the unpatterned waveguide (incidence angle θ).

and $\mathbf{K}_y$ are diagonal matrices whose diagonal coefficients are the components of vector $\mathbf{K}_{lm}$ and $\mathbf{E}$ is the Toeplitz matrix formed by the Fourier coefficient of the relative permittivity. Matrices $\boldsymbol{\epsilon}_x$ and $\boldsymbol{\epsilon}_y$, that are also formed by the Fourier coefficients of the relative permittivity, are not simply Toeplitz matrices; for more details see Ref. 10 where high convergence performance are reported for the computation of photonic band structures with the plane-wave method.

To integrate Eq. (2), the real continuous profile is approximated by a stack of slices with piecewise-constant permittivities, see Fig. 2(b). Within this approximation, the integration is done analytically; the modes and the propagating constants in every slice (p) are computed as the eigenvectors $\mathbf{W}_m^{(p)}$ and eigenvalues $\lambda_m^{(p)}$ of the corresponding matrices $\boldsymbol{\Omega}^{(p)}$. Thus, in each slice ($p$), the electromagnetic fields $\boldsymbol{\Psi}^{(p)}$ are looked on as a superposition of these modes

$$\boldsymbol{\Psi}^{(p)}(z)=\sum_m \mathbf{W}_m^{(p)}[b_m^{(p)}\exp(-\lambda_m^{(p)}z)+f_m^{(p)}\exp(\lambda_m^{(p)}z)], \quad (3)$$

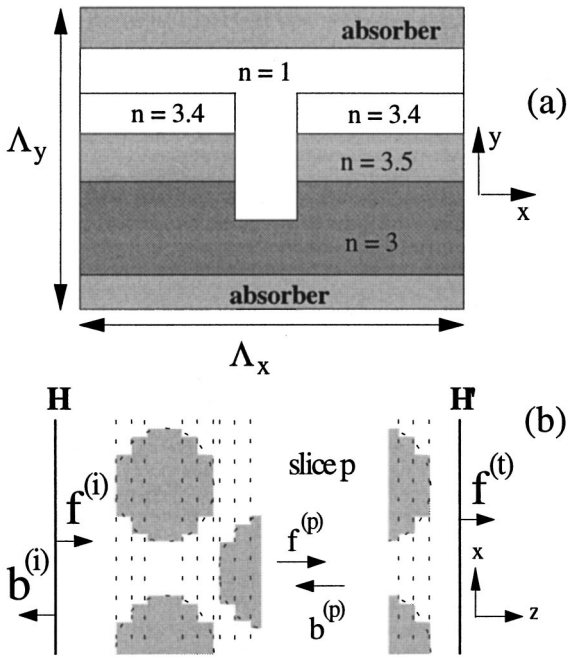

FIG. 2. (a) Artificial periodization along the vertical *y* direction with absorbers, see Ref. 9 for more details. (b) Slicing along the *z* direction.

where $\mathbf{b}^{(p)}$ and $\mathbf{f}^{(p)}$ are column vectors whose elements are the amplitudes of the modes propagating backward (in the $-z$ direction) and forward (in the z direction), respectively. Because of the linearity of Maxwell's equations, a matrix relationship between the mode amplitudes in the input medium (H plane) and those in the output medium (H' plane) exists. To avoid any numerical problems relative to the exponentially divergent terms in Eq. (3), a *S*-matrix (denoted $\mathbf{S}$) approach[11] is used to relate the amplitudes $\mathbf{b}^{(i)}$ (resp. $\mathbf{f}^{(t)}$) of the modes propagating backward (resp. forward) at the H (resp. H') plane to the amplitudes $\mathbf{f}^{(i)}$ of the modes propagating forward at the $\mathbf{H}'$ plane

$$\begin{bmatrix}\mathbf{b}^{(i)}\\ \mathbf{f}^{(t)}\end{bmatrix}=\mathbf{S}\begin{bmatrix}\mathbf{0}\\ \mathbf{f}^{(i)}\end{bmatrix}. \quad (4)$$

The zero vector of the bracket in the right side of Eq. (4) expresses the fact that no light is impinging on the ICPC from the output region ($\mathbf{b}^{(t)}=\mathbf{0}$). From the knowledge of the incident illumination $\mathbf{f}^{(i)}$, the reflected and transmitted intensities into the diffracted guided modes are derived from Eq. (4) by calculating the ratio between the time-averaged Poynting-vector z components of the diffracted modes and that of the fundamental incident mode.

The present method is tested against experimental results[12] obtained for ICPC fabricated by etching a planar monomode asymmetric waveguide. The waveguide is composed[12] of a GaAs (refractive index 3.5) 250 nm wide core with claddings with refractive indices 3.4 for the cover and 3.0 for the substrate. The cover thickness is 330 nm. The ICPC consists of a triangular array of holes with a lattice parameter a. We define by f the air fill factor (ratio of holes to total area). The holes are assumed to have straight sidewalls (perfect cylinders) and to have a finite depth h. The hole depth and the fill factor are the free parameters used for fitting the calculations to the experimental data.

For the numerical computations, we best match the experimental conditions and consider that the PC waveguide is illuminated under normal incidence ($\theta=0$) by the fundamental TE_0 mode of the waveguide. This mode is assumed to be perfectly collimated along the x direction. In the experiment, a maximum internal angle of $\theta=\pm 6°$ with respect to the z direction is collected. Moreover, in line with the experiment,[12] seven different lattice periods $a=180$, 200, 220, 240, 260, 280, and 300 nm and with identical fill factors are considered. Finally, two directions of propagation along the ΓM and ΓK principal crystallographic axis are investigated. For the ΓM and ΓK cases, the number of hole rows in the z direction are 8 and 15, respectively.

Figure 3 shows a comparison between the experimental (noisy curves) and the numerical (solid curves) transmission results as a function of the normalized frequency $u=a/\lambda$. For the ΓM direction, see Fig. 3(a), the seven lattice periods are shown. For the ΓK direction, see Fig. 3(b), only the three lattice periods $a=240$, 260, and 280 nm near the airband edge are shown. These three periods are crucial to quantify the radiation losses because, at the air-band edge, the field is localized inside the holes. For the calculation, we use a fill factor of $f=18\%$. This value controls the position of band edges. Then we assume that the hole depth is varying lin-

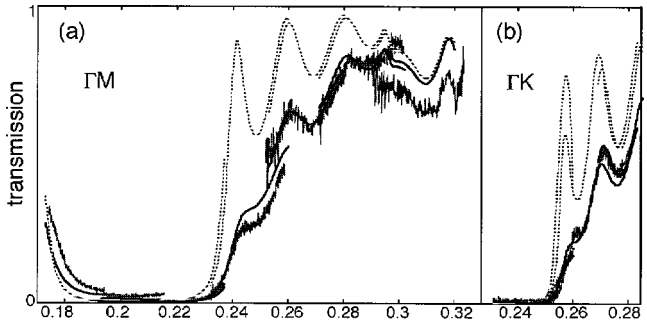

FIG. 3. Comparison between experimental transmission measurement (noisy curves) and theoretical predictions (solid curves). The dashed curves correspond to theoretical predictions for 800 nm deep holes.

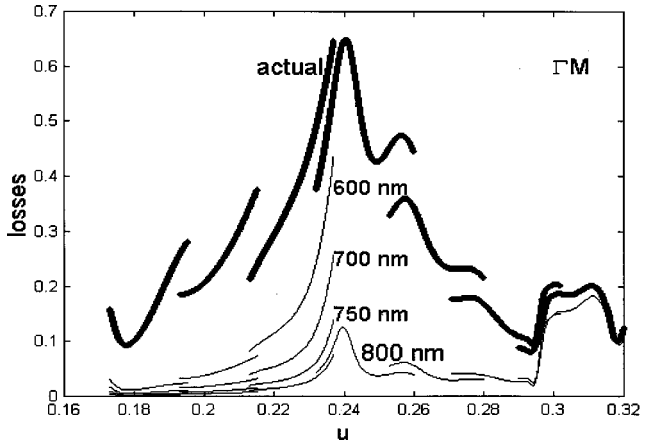

FIG. 4. Losses including in-plane diffraction: Thin curves: computational results anticipating ultimate performance for $h=800$ nm. Losses in the band gap are also shown for $h=600$, 700, and 750 nm. Bold curve: computed actual losses. The bumps for $u>0.295$ are due to in-plane diffraction.

early from one sample to the other: $h(a)=Ca+h_0$. This assumption (large holes are deeper than small ones) is reasonable with respect to the well-known properties of the reactive-ion-etching process used for the fabrication. With $h_0=155$ nm and $C=1.92$, the depth varies linearly from 500 nm for the 180 nm period sample to 731 nm for the sample with the largest period.

Essentially, an excellent agreement between the experimental and the numerical results is obtained. The band edges and the ripples on the sides of the gaps are correctly located for ΓM and ΓK propagation directions. The model is also able to predict quantitatively the losses induced by out-of-plane diffraction. The degree of radiation losses (mostly in the substrate) is basically dictated by the finite depth of the holes, and is extremely sensitive to this parameter, as was observed during the fitting procedure.

The model is able to quantitatively predict the losses achievable with holes etched deeper into the substrate for this specific waveguide. For $h=800$ nm, a realistic value with current etching techniques, we predict excellent performance as shown by the transmission dashed curves of Fig. 3 with a peak transmission of $\approx$90% at the air-band edge for the ΓM direction. For the ΓK direction, the 65% transmission at the air-band edge is smaller. This lower transmission is due to a high (25%) in-plane diffraction into the $\pm$ first orders. Figure 4 shows a comparison for the loss (a crucial quantity that is delicate to measure) between the actual performance and anticipated performance for deeper holes. In view of the different results, it is reasonably predicted that the ultimate intrinsic losses in the band gap for $0.18<u<0.22$ are reached for a 800 nm hole depth. In Fig. 4, the losses include not only the out-of-plane scattering but also the in-plane diffraction into the transmitted and reflected positive- and negative-first diffracted guided waves. Note however that this in-plane diffraction appears only for $u>0.295$ as shown by the loss bump in Fig. 4. More impressive is the performance achieved in the band gap; over a wide frequency interval from 0.185 to 0.215, the losses for $h=800$ nm are smaller than 1%. In this interval, the reflectivity exceeds 98%. One obvious consequence of this high reflectivity with small intrinsic losses is the feasibility of microcavities with Q factor larger than 5000, that can have a great impact on future all-optical telecommunication photonic crystals.

The model presented here to estimate the ultimate performance of photonic crystals etched through waveguides is versatile. The *S*-matrix approach can be applied to any index-confined photonic crystal, with arbitrary heterostructure, atom shape and mirror size. It can also address in-plane photonic-crystal cavities (line defects in Ref. 7). Validation by the experimental data of Refs. 3–4 shows that, in revision of Ref. 12, the hole depth is the limiting factor to the performance of these particular ICPC. Conversely, the results indicate that ultimate performances could be attained for $h=800$ nm etch depth, with losses of no more than 1% in the gap, confirming the good potential of 2D photonic crystal etched through conventional waveguides.

Part of this work is supported under the Information Society Technology contract PCIC. The authors acknowledge Claude Weisbuch for fruitful discussions, and Christopher Smith and Thomas Krauss from the University of Glasgow for fabricating the ICPC used in this work to test the model.

[1] J. D. Joannopoulos, P. R. Villeneuve, and S. Fan, Science **386**, 143 (1997).
[2] T. F. Krauss, R. M. De La Rue, and S. Brand, Nature (London) **383**, 699 (1996).
[3] D. Labilloy *et al.*, Phys. Rev. Lett. **79**, 4147 (1997); D. Labilloy, H. Benisty, C. Weisbuch, C. J. M. Smith, T. F. Krauss, R. Houdré, and U. Oesterle, Phys. Rev. B **59**, 1649 (1999).
[4] H. Benisty *et al.*, J. Lightwave Technol. **17**, 2063 (1999).
[5] O. J. Painter, A. Husain, A. Scherer, J. D. O'Brien, I. Kim, and P. D. Dapkus, J. Lightwave Technol. **17**, 2082 (1999).
[6] M. Tokushima, H. Kosaka, A. Tomita, and H. Yamada, Appl. Phys. Lett. **76**, 952 (2000).
[7] B. d'Urso, O. Painter, J. O'Brien, T. Tombrello, A. Yariv, and A. Scherer, J. Opt. Soc. Am. B **15**, 1155 (1998).
[8] L. Li, J. Opt. Soc. Am. A **14**, 2758 (1997).
[9] P. Lalanne and E. Silberstein, Opt. Lett. **25**, 1092 (2000).
[10] Ph. Lalanne, Phys. Rev. B **58**, 9801 (1998).
[11] N. P. K. Cotter, T. W. Preist, and J. R. Sambles, J. Opt. Soc. Am. A **12**, 1097 (1995).
[12] H. Benisty, D. Labilloy, C. Weisbuch, C. J. M. Smith, T. F. Krauss, D. Cassagne, A. Béraud, and C. Jouanin, Appl. Phys. Lett. **76**, 532 (2000).